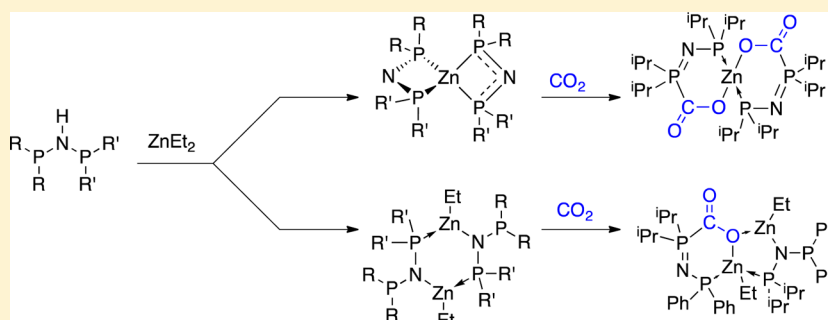


Structures and CO₂ Reactivity of Zinc Complexes of Bis(diisopropyl)- and Bis(diphenylphosphino)aminesDiane A. Dickie[†] and Richard A. Kemp^{*,†,‡}[†]Department of Chemistry and Chemical Biology, University of New Mexico, Albuquerque, New Mexico 87131, United States[‡]Advanced Materials Laboratory, Sandia National Laboratories, Albuquerque, New Mexico 87106, United States

Supporting Information



ABSTRACT: The bis(phosphino)amines (R₂P)NH(PR')₂ (R = R' = isopropyl; R = R' = phenyl; R = isopropyl, R' = phenyl) react with ZnEt₂ to form complexes with two different structural motifs, either the homoleptic monomeric P,P-chelates Zn[N(i-Pr₂P)₂]₂ and Zn[N(i-Pr₂P)(Ph₂P)]₂ or the heteroleptic dimeric Zn₂N₂P₂ heterocycles {EtZn[N(PPh₂)₂]}₂ and {EtZn[N(PPh₂)(i-Pr₂P)]}₂. In two cases, CO₂ reacts with these complexes to give adducts Zn[O₂CP(i-Pr₂)NP(i-Pr₂)]₂ and Zn[O₂CP(i-Pr₂)NPPh₂][Ph₂PN(i-Pr₂P)]ZnEt₂, similar to adducts formed from the reaction of CO₂ with frustrated Lewis pairs (FLPs). In the other two cases, reaction with CO₂ results in cleavage and rearrangement of the N–P bonds to give either N(PPh₂)₃ or Ph₂P(iPr₂P)NPPh₂. The zinc complexes and their CO₂ products were characterized with a combination of single crystal X-ray diffraction and multinuclear NMR spectroscopy.

INTRODUCTION

The quest for molecules and methods that will facilitate the chemical, electrochemical or biochemical reduction of carbon dioxide to rebalance the global carbon cycle is an important and growing field of research.¹ CO₂ has long been known to insert into a variety of highly polarized M–E bonds (E = H, CR₃, NR₂, OR), but until the development of the “frustrated Lewis pair” (FLP) concept, insertion into M–P bonds was rare. The term FLP was coined by Stephan² in 2007 to describe complexes in which a highly Lewis acidic borane and a Lewis basic phosphine are prevented by sterics from interacting directly with one another and are thus primed to react with small molecules. Because CO₂ has both nucleophilic and electrophilic sites, it is an ideal molecule for releasing the “frustration” of the Lewis pair, and FLPs have become prominent in CO₂ activation. The resulting complexes are typically described as CO₂-adducts and show an average O–C–O bond angle³ of 126°, closely resembling the geometry required to use CO₂ in a reduced form as a C₁ source for fuels or other value-added products.

Similar reactivity, both catalytic and stoichiometric, has since been reported for a variety of main group and transition metal Lewis acids, including many that exist as traditional unfrustrated coordination complexes.⁴ For example, upon exposure to CO₂, the P,P-chelated Sn(II) complex [(i-Pr₂P)₂N]₂Sn reversibly

forms an adduct with one P atom of each ligand (two CO₂ per Sn).⁵ This tin complex was the first structurally characterized example featuring the monoanionic ligand [(i-Pr₂P)₂N][−], even though it is the precursor for the widely used oxidized ligands [i-Pr₂P(X)NP(i-Pr)₂][−] and [(i-Pr₂P(X))₂N][−] (X = O, S, Se, Te).³ A similar discrepancy in the application of the oxidized vs nonoxidized (P^v vs P^{III}) ligands is seen in the closely related [(Ph₂P)₂N][−] system. There are more than 350 structurally characterized metal complexes of the fully or partially oxidized monoanionic phenyl-substituted ligand, significantly more than the nonoxidized form.³

Ligands of the general form [(R₂P)₂N][−] have the potential to be highly versatile because both N and P can act as donors to a metal, while still maintaining an open Lewis basic site for reaction with CO₂ or other small molecules. Figure 1 summarizes the coordination modes that have been reported in structurally characterized compounds of this general class and the approximate number of examples of each.³ Modes B and D are predominately seen in transition metal complexes, while main group and rare earth metals generally favor coordination to the harder nitrogen atom. Herein we describe the synthesis and structural characterization of Zn complexes of

Received: August 22, 2014

Published: November 3, 2014

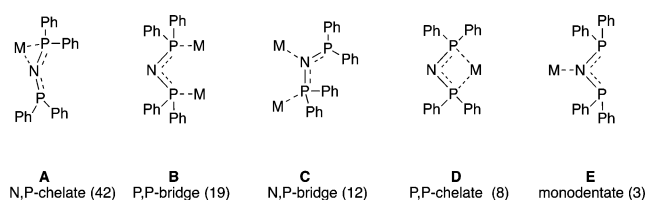


Figure 1. Coordination modes of structurally characterized metal complexes of $[(\text{Ph}_2\text{P})_2\text{N}]^-$. The number in parentheses indicates the number of examples found in the CSD.³

three different $[(\text{R}_2\text{P})_2\text{N}]^-$ ligands which were found to coordinate via modes C and D, and the reactivity of these complexes with CO_2 .

RESULTS AND DISCUSSION

Ligand synthesis and structure. The syntheses and structures of the ligands $(i\text{-Pr}_2\text{P})_2\text{NH}$ **1**⁵ and $(\text{Ph}_2\text{P})_2\text{NH}$ **2**⁶ have been described elsewhere. The new mixed alkyl/aryl ligand $(i\text{-Pr}_2\text{P})\text{NH}(\text{PPh}_2)$ **3** was prepared by the addition of one equivalent of Ph_2PCl to a toluene solution of $(i\text{-Pr}_2\text{P})\text{NH}(\text{SiMe}_3)$.⁷ After stirring at room temperature for 90 min, the solvent and the chlorotrimethylsilane coproduct were removed under vacuum to leave the white solid **3**. The ³¹P NMR spectrum of **3** showed two doublets with a ²J_{PP} coupling of 179 Hz. The signal assigned to the *i*-Pr₂P group appeared at 72.1 ppm while the PPh₂ group was found at 40.7 ppm. These chemical shifts were slightly downfield and upfield, respectively, from the homoleptic molecules **1** (68.0 ppm) and **2** (44.3 ppm).

X-ray quality single crystals of **3** can be grown from THF solution at -25°C . Figure 2 shows the two crystallographically

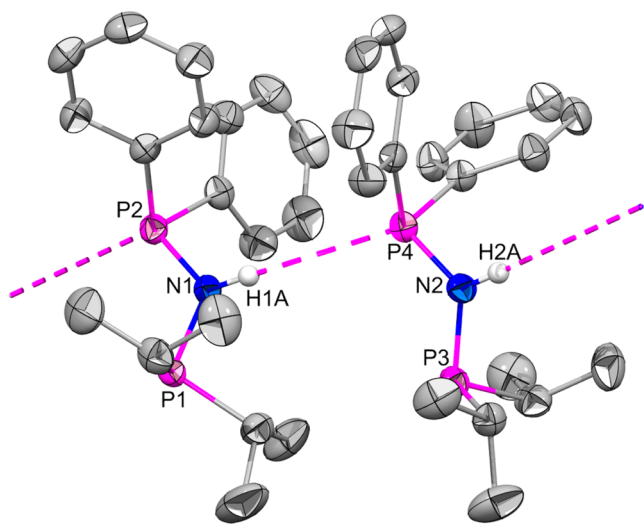


Figure 2. Structure of **3**. Thermal ellipsoids are shown at 50% probability. For clarity, only N–H hydrogens are shown.

distinct molecules in the asymmetric unit. The phosphorus atoms exhibit a pyramidal geometry, while both nitrogen atoms are planar ($\sum\angle_{\text{N1}} = 358.36^\circ$; $\sum\angle_{\text{N2}} = 358.71^\circ$). Each amine hydrogen points directly ($\angle\text{N1-H1A}\cdots\text{P4} = 179.03^\circ$; $\angle\text{N2-H2A}\cdots\text{P2} = 178.03^\circ$) at the lone pair of the other molecule's phenyl-substituted phosphorus atom. Given that geometry, it is tempting to describe these as N–H \cdots P hydrogen bonds, but the rather long distances involved ($\text{N1}\cdots\text{P4} = 3.982 \text{ \AA}$; $\text{N2}\cdots\text{P2}$

$= 3.996 \text{ \AA}$) suggest that these are extremely weak interactions.⁸ The N–P_{Ph} bonds (Table 1) are shorter ($\text{N1-P2} = 1.6908(13) \text{ \AA}$; $\text{N2-P4} = 1.6924(13) \text{ \AA}$) than the N–P_{*i*Pr} bonds ($\text{N1-P1} = 1.7111(13) \text{ \AA}$; $\text{N2-P3} = 1.7117(13) \text{ \AA}$), consistent with the bond lengths in the homoleptic complexes, which average $1.705(4) \text{ \AA}$ for **1**⁵ and $1.692(2) \text{ \AA}$ for **2**.^{6a,c} The P–N–P angles in **3** measure $120.76(8)$ and $120.81(8)^\circ$, intermediate between the angles for **1** [$121.2(2)$ and $121.3(2)^\circ$]⁵ and **2** ($118.9(2)^\circ$ ^{6a} or 118.86° ^{6c}).

Syntheses and structures of Zn complexes. Addition of diethylzinc to a pentane solution of **1** (Scheme 1) results in the loss of two equivalents of ethane and formation of $[(i\text{-Pr}_2\text{P})_2\text{N}]_2\text{Zn}$ **4** as a colorless, crystalline solid in very good yield. The ³¹P{¹H} spectrum showed a single peak at δ 91.4 ppm, more than 20 ppm downfield from the free ligand **1**, which is found at 68.0 ppm. This chemical shift is strongly suggestive of P,P-chelation (Figure 1, mode D), the same coordination pattern seen in the tin analog $[(i\text{-Pr}_2\text{P})_2\text{N}]_2\text{Sn}$.⁵

The P,P-chelation mode of **4** was confirmed by single-crystal X-ray diffraction (Figure 3). In **4**, the geometry at Zn is distorted tetrahedral, with the two ZnP₂N rings oriented at an angle of $88.70(5)^\circ$ from one another. The P–N bonds are much shorter and the P–N–P angles more acute in **4** than in the free ligand **1**⁵ (Table 1). This is consistent with an allylic P–N–P bonding description, with the monoanionic charge delocalized across the three heteroatoms of each ligand.

In contrast to the virtually unexplored coordination chemistry of **1**, ligand **2** has been shown to exhibit at least five different coordination modes (Figure 1) with a variety of main group, transition metal, and lanthanide elements. Therefore, it was not clear a priori whether the reaction of **2** with diethylzinc would yield an analog of **4** or an entirely different structural motif. A variety of conditions and metal/ligand ratios were screened, and in all cases the same product **5** was obtained. Multinuclear NMR spectroscopy showed a single peak at 49 ppm in the ³¹P spectrum, while the ¹H and ¹³C spectra suggested a heteroleptic complex consistent with one ethyl group remaining bound to the Zn atom. The optimized conditions for the formation of **5** (Scheme 1) were found to be an overnight reaction at rt of an equimolar combination of **2** and ZnEt₂ in toluene.

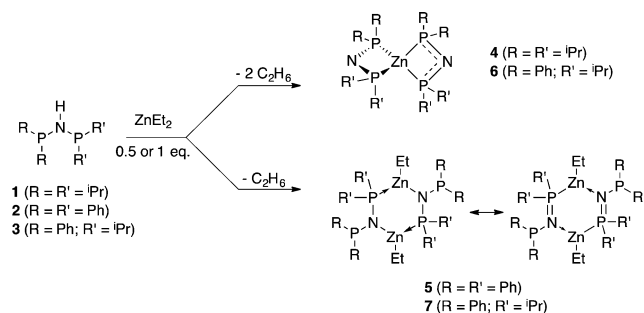
Single crystals of **5** were grown from a combination of THF, pentane, and toluene. X-ray diffraction (Figure 4) revealed that two of those solvents, toluene and THF, were incorporated into the crystal lattice, and an additional molecule of THF was coordinated to Zn1. The ligand acts as an N,P-bridge (Figure 1, mode C) between two different Zn centers giving a six-membered boat-like Zn₂N₂P₂ ring. This dimeric heterocyclic motif has been previously reported. In three of the known examples,⁹ the multidentate ligands engage in additional interactions besides the main heterocycle. That is in contrast to **5**, in which the second P atom of each ligand remains free. This makes its structure more comparable to the remaining two literature examples, both of which feature bidentate ligands of the general form $-\text{N}(\text{PR}_2)(\text{SiMe}_3)$.¹⁰

The Zn–N bonds ($\text{Zn1-N1} = 1.993(3)$; $\text{Zn2-N2} = 1.983(3) \text{ \AA}$) are near the average for other EtZn-amido complexes in the CSD (mean Zn–N = 1.995 \AA), which suggests significant covalent character in that bond. An examination of the N–P bonds, however, indicates that the N= P resonance form shown in Scheme 1 likely also contributes. As summarized in Table 1, the endocyclic N–P bonds of **5** are significantly shorter ($\text{N1-P2} = 1.659(3)$; N2-P3

Table 1. Selected Bond Lengths (Å) and Angles (deg) for Ligands 1–3 and Zn Complexes 4–7

	Ligands			
	1 ^s		2 ^{6c}	3
N–P _{iPr}	1.704(4)–1.706(4)			1.7111(13)–1.7117(13)
N–P _{Ph}			1.692(2)	1.6908(13)–1.6924(13)
P–N–P	121.2(2)–121.3(2)		118.9(2)	120.76(8)–120.81(8)
Zn complexes				
	4	5	6	7
N–P _{iPr}	1.6403(17)–1.6483(18)		1.6496(19)–1.6532(19)	1.669(2)–1.674(3) endo
N–P _{Ph}			1.6402(19)–1.6419(19)	1.700(3)–1.707(3) exo
Zn–P _{iPr}	2.4184(6)–2.4291(5)		2.3776(6)–2.3829(6)	2.4344(9)–2.4438(9)
Zn–P _{Ph}			2.4106(6)–2.4213(6)	
Zn–N	1.983(3)–1.993(3)			1.976(3)–1.981(3)
P–N–P	107.87(9)–108.57(9)		107.02(10)–107.07(10)	120.60(16)–121.00(16)
CO ₂ adducts				
	8		11	
N–P _{iPr/CO2}	1.577(2)–1.582(3)		1.579(2)	
N–P _{iPr}	1.624(3)–1.636(2)		1.679(2)	
N–P _{Ph}			1.632(2) endo 1.719(2) exo	
Zn–P _{iPr}	2.3387(9)–2.3432(8)		2.4160(7)	
Zn–P _{Ph}			2.4108(7)	
Zn–O	1.982(2)–2.003(2)		2.1245(18)–2.1741(18)	
C–O _{Zn}	1.256(4)–1.275(4)		1.288(3)	
C–O	1.217(4)–1.224(4)		1.227(3)	
P–N–P	130.58(17)–132.22(15)		119.03(13)–131.82(14)	
O–C–O	126.6(3)–127.3(3)		125.2(2)	

Scheme 1. Synthesis of Zn Complexes 4–7



P4 = 1.662(3) Å) than the free ligand 2 (1.692(2) Å), and the exocyclic N–P bonds (N1–P1 = 1.719(3); N2–P3 = 1.711(3) Å) are longest of all.

Given the dramatic difference in the coordination modes observed in 4 and 5, it was of great interest to explore the behavior of 3 with ZnEt₂. For reasons of solubility, the initial screening reaction was performed in toluene. The reaction was monitored by ³¹P{¹H} NMR over the course of several days. The final product, 6, displayed a pair of doublets in the ³¹P spectrum at 100.1 and 61.3 ppm, with ²J_{PP} = 300 Hz. The large downfield shift of the signals relative to the starting ligand 3 was much more comparable to the change between 1 and 4 than between 2 and 5, suggesting that 6 had adopted a P,P-chelate structure (Figure 1, mode D). The ¹H and ¹³C{¹H} spectra of 6 obtained after the product had been isolated showed no evidence of the zinc-ethyl group, which was also consistent with a P,P-chelate.

Single crystals of 6 were grown from THF and X-ray diffraction (Figure 5) confirmed that 6 had the same coordination mode as 4. The geometry at Zn1 is a distorted

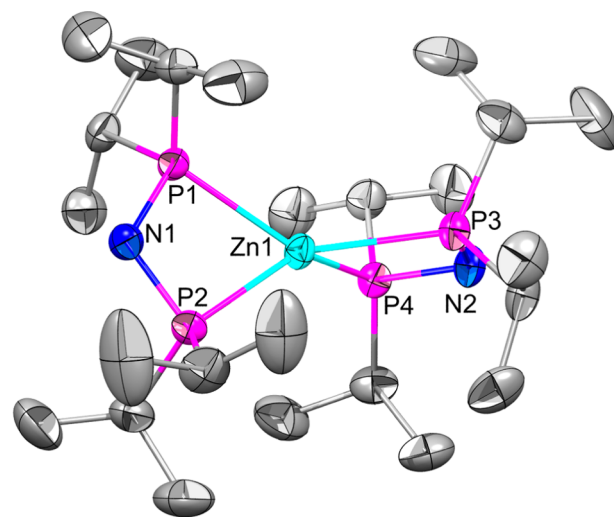


Figure 3. Structure of 4. Thermal ellipsoids are shown at 50% probability. For clarity, H atoms are not shown.

tetrahedron, with an angle of 87.53(5)° between the two ZnP₂N rings. The allylic nature of the anionic PNP fragment is shown by the shortened, equalized N–P bonds (Table 1). The fact that they are the same within experimental error is somewhat surprising, given how different the N–P_{iPr} and N–P_{Ph} bond lengths are in the free ligand 3. In contrast to the N–P bonds, there is a difference in the Zn–P bonds. The Zn–P_{iPr} bonds in 6 measure 2.3776(6) and 2.3829(6) Å, shorter than the same bonds in 4 and shorter than the Zn–P_{Ph} bonds in either 5 or 6.

As mentioned above, the initial synthesis of 6, which was later optimized to a few hours of reflux in toluene, was first

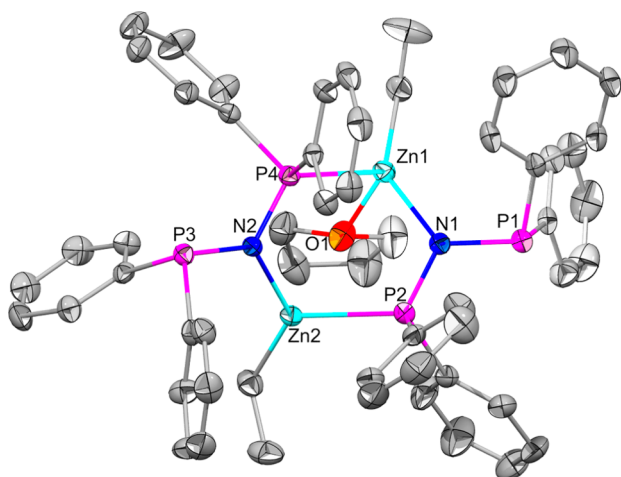


Figure 4. Structure of 5. Thermal ellipsoids are shown at 50% probability. For clarity, H atoms and noncoordinated solvent molecules are not shown.

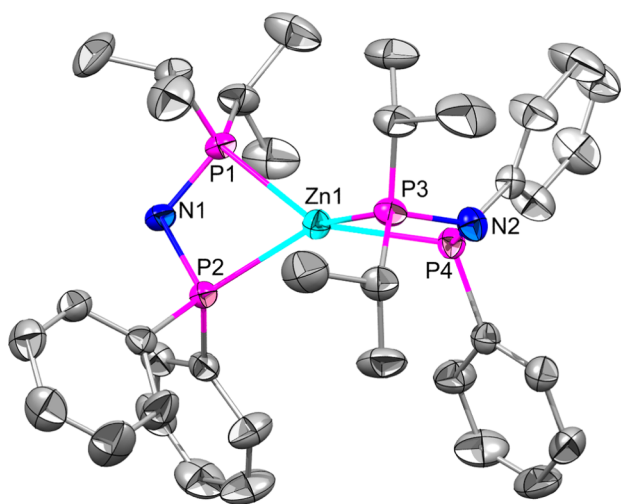


Figure 5. Structure of 6. Thermal ellipsoids are shown at 50% probability. For clarity, H atoms are not shown.

performed at rt over several days. During the monitoring of that reaction by $^{31}\text{P}\{^1\text{H}\}$ NMR spectroscopy, formation of an intermediate 7 was observed. Two different signals were present in the spectrum, but in contrast to the P–P coupled doublets of 3 and 6, complex 7 gave rise to singlets. While it is possible to isolate 7 from the reaction leading to 6, higher yields without traces of 3 or 6 were much easier to achieve from a rational synthesis based on the reaction of equimolar amounts of 3 and ZnEt_2 in pentane. With that clean product in hand, further characterization was performed and 7 was found to be an analog of the heterocyclic dimer 5.

Because the chemical shift assigned to the P_{iPr} in the $^{31}\text{P}\{^1\text{H}\}$ NMR spectrum of 7 is nearly identical to that of 3 at 71.4 and 72.1 ppm, respectively, and the P_{Ph} signal had shifted from 40.7 ppm in 3 to 52.2 ppm in 7, we initially thought that the exocyclic group was the former and the endocyclic the latter. Single crystal diffraction studies (Figure 6) later revealed that the opposite was true—it is the P_{iPr} that is bound to Zn, and the P_{Ph} that is free. As in 5, the endocyclic N–P bonds (Table 1) in 7 are much shorter than the exocyclic bonds. Despite the dramatic changes in bond lengths, the P–N–P angles in both 5

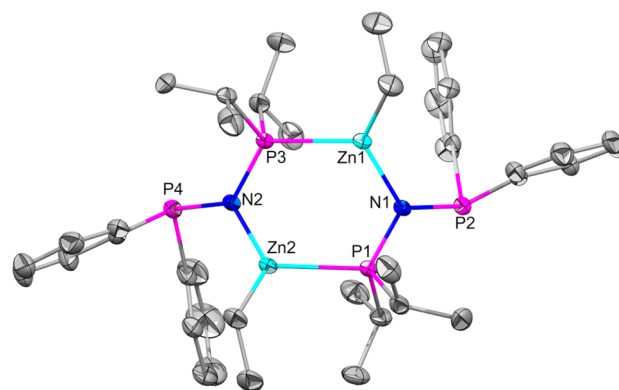
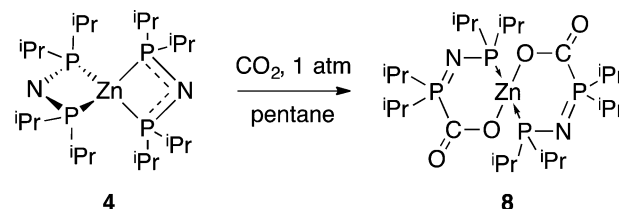


Figure 6. Structure of 7. Thermal ellipsoids are shown at 50% probability. For clarity, H atoms and noncoordinated THF solvent are not shown.

and 7 are identical to those measured in the free ligands 2 and 3, respectively.

Reactivity of Zn complexes with CO_2 . When CO_2 is bubbled through a pentane solution of 4, a white precipitate 8 is formed within a few minutes (Scheme 2). Two pieces of data

Scheme 2. Reaction of CO_2 with 4 To Give Adduct 8



are characteristic of the formation of CO_2 adducts—the $\nu(\text{C}=\text{O})$ stretch in the IR spectrum and the downfield doublet in the $^{13}\text{C}\{^1\text{H}\}$ NMR spectrum. The IR spectrum of the Zn product 8 showed a very strong CO stretch at $\nu = 1633\text{ cm}^{-1}$, close to that observed for the Sn analog (1626 cm^{-1}),⁵ and well within the range of what has been previously reported for P-based frustrated Lewis pair (FLP) adducts ($\nu = 1608\text{--}1702\text{ cm}^{-1}$).¹¹ A phosphorus-coupled doublet assigned to coordinated CO_2 was observed in the $^{13}\text{C}\{^1\text{H}\}$ NMR at 168.8 ppm with a $^1\text{J}_{\text{CP}}$ coupling of 90 Hz. Again, this is comparable to both the Sn analog (168.7 ppm, $^1\text{J}_{\text{CP}} = 95\text{ Hz}$)⁵ and the known FLP-adducts.^{11,12} Both the ^1H and $^{13}\text{C}\{^1\text{H}\}$ spectra of 8 show distinct sets of signals for the isopropyl groups on the CO_2 -bound P and the Zn-bound P, with the CO_2 set distinctly broadened. The $^{31}\text{P}\{^1\text{H}\}$ NMR spectrum of 8 confirmed the presence of inequivalent P atoms, displaying two singlets with no discernible P–P coupling at $\delta = 31.6$ and 45.8 ppm.

In addition to the spectroscopic characterization, single crystal diffraction studies were performed on 8 (Figure 7). Two crystallographically independent molecules were found in the triclinic unit cell. The Zn–P bonds (Table 1) in the adduct 8 are nearly 0.1 Å shorter than in the starting complex 4, and the P–N bonds are no longer allylic. Instead, there are distinct shorter (1.577(2)–1.582(2) Å) and longer (1.624(3)–1.636(2) Å) P–N bonds in each of the four ligands, with the shorter bonds associated with the CO_2 -bound P. The C–O bonds within each CO_2 fragment differ, with the O bound to the metal showing more single bond character and the pendant O more double bond character. The geometry at Zn remains a

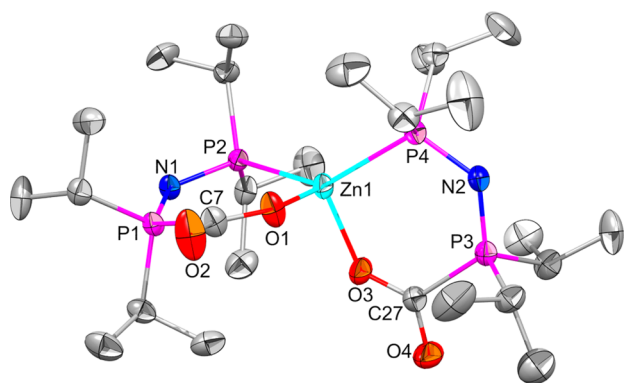


Figure 7. Structure of **8**. For clarity, only one of two crystallographically independent molecules is shown and H atoms were omitted.

distorted tetrahedron in **8** and the six-membered CO₂-containing rings are offset from one another by 88.54(7)° for the Zn1 molecule and 88.13(7)° for Zn2. The process of going from four-membered ZnP₂N rings in **4** to six-membered rings in the CO₂ adduct **8** allows the P–N–P bond angles to increase by more than 20° to an average of 131° while the O–C–O fragments are bent to an average 127°.

As was described above, there are only a few six-membered Zn₂N₂P₂ heterocycles similar to **5** in the literature. One of these, based on the ligand -N[P(*i*-Pr₂)(SiMe₃)], has been shown to form an adduct very similar to **8** although the mechanism for its formation is somewhat more complicated than simple insertion into a Zn–P bond.^{10b} Therefore, it was expected that the reaction of **5** with CO₂ would also give a CO₂-inserted product, but likely not cleanly. It was somewhat surprising, therefore, to find that upon bubbling carbon dioxide through a toluene solution of **5**, only a single phosphorus-containing product was observed by ³¹P{¹H} NMR at 59 ppm. The IR spectrum of the isolated powder, **9**, did not show any stretches characteristic of CO₂ insertion. Single crystals of **9** were grown and were found to be the tertiary amine N(PPh₂)₃.¹³ We have been unable to determine the fact of Zn in this reaction. We have previously reported the cleavage and rearrangement of N–P bonds in the presence of CO₂ to give **9** and/or its isomer Ph₂P(Ph₂P)NPPPh₂,¹⁴ and similar oxidative scrambling of the [N(PPh₂)₂][−] ligand under a variety of conditions has been reported by others.¹⁵

Despite its structural similarity with **4**, solutions of **6** in either pentane or toluene showed no reaction with CO₂ under the time, temperature and pressure conditions used for **4** and **5**. Upon switching to the polar solvent THF, however, spectroscopic evidence for a reaction was observed. A strong stretch in the IR spectrum grew in at 1639 cm^{−1}, while the ³¹P{¹H} NMR collapsed to two broad singlets at 34.9 and 21.3 ppm. These data are consistent with the formation of a CO₂-adduct similar to **8**, but in this case it was not isolable. Instead, the product that was ultimately obtained from the reaction was more closely related to **9**. It was possible to identify **10** as Ph₂P(*i*Pr₂P)NPPPh₂ by both ³¹P{¹H} NMR and single crystal X-ray diffraction (Figure 8). The central isopropyl-substituted phosphorus atom has the most downfield chemical shift at 44.5 ppm and appears as a doublet of doublets with couplings of 267 Hz to its directly bound neighbor at −29.7 ppm, and 82 Hz to the N-bound phosphorus atom at 39.7 ppm. The NMR pattern

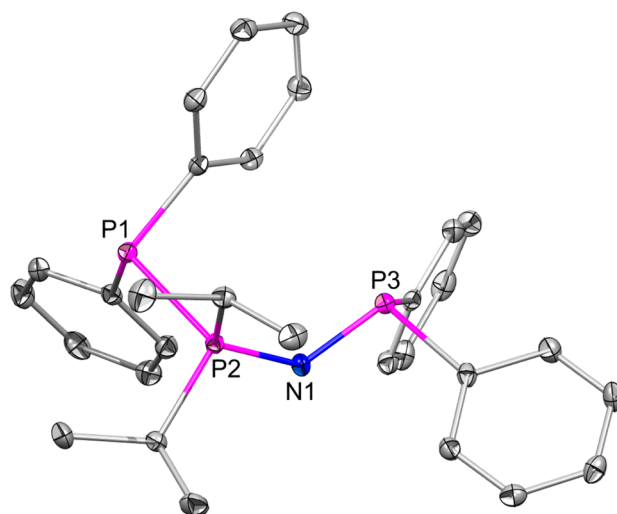
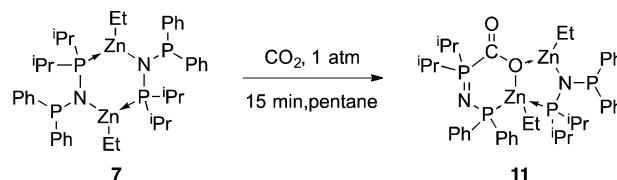


Figure 8. Structure of **10**. Thermal ellipsoids are shown at 50% probability. For clarity, H atoms are not shown. Selected bond lengths (Å) and angles (deg): P1–P2 = 2.2352(5), P2–N1 = 1.5876(13), N1–P3 = 1.6778(13), P1–P2–N1 = 120.98(5), P2–N1–P3 = 125.78(8).

and the structural parameters of **10** are very similar to those of the previously published Ph₂P(Ph₂P)NPPPh₂,^{14a} an isomer of **9**.

Finally, the reaction of **7** with CO₂ was explored. Because **5**, **6** and the related group 2 complexes¹⁴ had all undergone some form of N–P_{ph} bond cleavage in the presence of CO₂, and because Zn₂N₂P₂ heterocyclic dimers have also been shown to disproportionate under similar conditions,^{10b} a complex mixture of products was anticipated from this reaction (Scheme 3). Upon bubbling CO₂ through a pentane solution of **7**, a

Scheme 3. Reaction of CO₂ with **7** to give **11**



white precipitate **11** was obtained. The stretch at 1634 cm^{−1} in the IR spectrum was strong evidence that **11** was a CO₂ insertion product. Unfortunately, no signal for this moiety was observed in the ¹³C NMR spectrum. The alkyl and aryl regions of the ¹H and ¹³C{¹H} NMR spectra were complicated, but suggested that the ethyl group was still present on zinc. These spectra also indicated that there was little symmetry in the product molecule. This was consistent with the ³¹P{¹H} NMR spectrum that showed four different phosphorus environments.

In order to elucidate the structure of **11**, single crystals were grown by vapor diffusion of pentane into a concentrated toluene solution. The structure (Figure 9) was consistent with the unsymmetric molecule suggested by the NMR data. One of the two ligands present in the starting material **7** retained its original coordination mode, binding to one zinc atom of the dimer through nitrogen and to the other through isopropyl-substituted phosphorus. The CO₂ molecule was found to have inserted itself into the Zn–P_{iPr} bond of the other ligand, with the bound oxygen bridging both Zn atoms. The retained ethyl groups, and rearrangement of the CO₂-bound ligand to

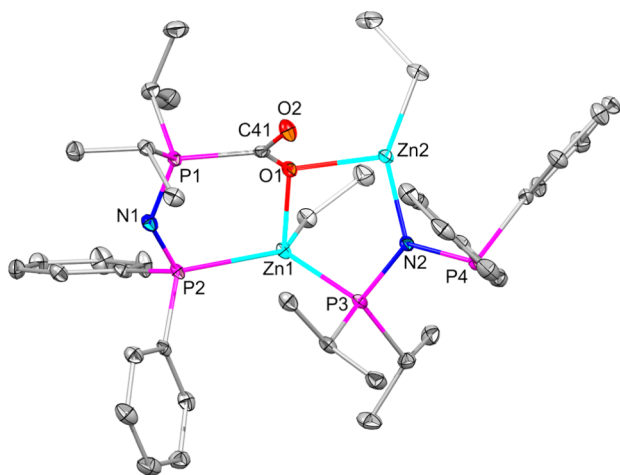


Figure 9. Structure of **11**. Thermal ellipsoids are shown at 50% probability. For clarity, H atoms are not shown.

coordinate through the phenyl-substituted P instead of through N, completed the coordination sphere of the Zn atoms.

The Zn–O bonds in **11** are longer (2.1245(18)–2.1741(18) Å) than in **8** (1.982(2)–2.003(2) Å), as is expected for a bridging O atom, while the C–O and C=O bonds of **8** and **11** are the same within experimental error. Upon binding CO₂, the N–P bond decreases by 0.1 Å compared to **7** and the “unreacted” side of **11**. Instead, it is in the middle of the range of bond lengths measured for the N–P bonds in **8**. Nearly as big a difference is observed with the endo- and exocyclic N–P bonds, with the exo being slightly longer (1.719(2) Å) than in **7** (1.700(3)–1.707(3) Å) and the endo being shorter (1.632(2) Å) than in **6**. Taken together, this suggests that the P1–N1–P2 fragment has more allylic character than in **8**. It is not surprising that a second molecule of CO₂ does not insert into the remaining Zn–P_{IPr} bond because the newly formed five-membered Zn–O–Zn–N–P ring should be stable and unstrained.

CONCLUSIONS

We have prepared and characterized four complexes from the reaction of ZnEt₂ with (*i*-Pr₂P)₂NH, (Ph₂P)₂NH and (*i*-Pr₂P)NH(PPh₂). As the substituent on phosphorus is changed from isopropyl to phenyl, the coordination mode of the ligand also changes. Coordination through phosphorus is favored for alkyl substituents, while aryl groups also permit coordination through N. This difference in donor ability is supported by recent calculations by Chivers et al. on the nucleophilicity of (R₂P)₂NH ligands.¹⁶ Two different structural motifs were obtained, either a P,P-chelated, disubstituted monomer, or a Zn₂N₂P₂ monosubstituted heterocycle. The all-isopropyl chelate and the mixed *i*Pr/Ph heterocycle both react with CO₂ via insertion into a P–Zn bond. In contrast, the mixed *i*Pr/Ph chelate and the all-phenyl heterocycle undergo N–P bond cleavage in the presence of CO₂ to form Ph₂P(*i*Pr₂P)NPPH₂ and N(PPh₂)₃, respectively, as had been previously seen for group 2 complexes of [(Ph₂P)₂N][−] under similar conditions.¹⁴

EXPERIMENTAL SECTION

General experimental. All manipulations were carried out in an argon-filled glovebox or by using standard Schlenk techniques. Ligands **1**⁵ and **2**^{6b} were prepared according to literature procedures.

Anhydrous solvents were stored in the glovebox over 4 Å molecular sieves prior to use. ¹H and ¹³C{¹H} spectra were referenced to residual solvent downfield of TMS. ³¹P{¹H} spectra were referenced to external 85% H₃PO₄. IR spectra were recorded as mulls or thin films on KBr windows. Single-crystal X-ray diffraction studies were performed on a Bruker Kappa Apex II CCD diffractometer. Crystals were coated in Paratone-N oil and mounted on either a CryoLoop or MiTeGen MicroLoop. The Bruker Apex2 software suite was used for data collection, structure solution and refinement. Relevant parameters are summarized in Tables S1 and S2 (Supporting Information).

HN(*i*-Pr₂P)(Ph₂P) (3). A solution of chlorodiphenylphosphine (1.07 g, 4.87 mmol) in ca. 15 mL toluene was added dropwise to a solution of N-trimethylsilyl-N-diisopropylphosphinoamine⁷ (1.00 g, 4.87 mmol) in ca. 10 mL toluene. The resulting slightly cloudy, pale yellow solution was stirred at rt for 90 min, then the solvent was removed under vacuum to give a white powder. Yield = 1.41 g (91%), mp = 101–102 °C. X-ray quality single crystals were grown from a concentrated THF solution. ¹H NMR (C₆D₆, 300 MHz) δ 0.93 (dd, ³J_{HP} = 10.9 Hz, ³J_{HH} = 6.9 Hz, 6H, CH(CH₃)₂), 0.94 (dd, ³J_{PH} = 14.8 Hz, ³J_{HH} = 6.9 Hz, 6H, CH(CH₃)₂), 1.50 (sept of d, ²J_{HP} = 2.4 Hz, ³J_{HH} = 6.9 Hz, 2H, CH(CH₃)₂), 2.17 (dd, ²J_{HP} = 8.6 Hz, ²J_{HP} = 5.5 Hz, 1H, NH), 7.02–7.13 (overlapping m, 6H, aryl H), 7.40–7.46 (overlapping m, 4H, aryl H) ppm. ¹³C{¹H} NMR (CD₂Cl₂, 75 MHz) δ 17.1 (d, ²J_{PC} = 8.4 Hz, CH(CH₃)₂), 18.7 (d, ²J_{PC} = 19.9 Hz, CH(CH₃)₂), 27.2 (dd, ¹J_{PC} = 14.5 Hz, ³J_{PC} = 8.3 Hz, CH(CH₃)₂), 128.2 (d, ³J_{PC} = 6.5 Hz, meta-C), 128.7 (s, para-C), 130.9 (d, ²J_{PC} = 21.1 Hz, ortho-C), 143.7 (dd, ¹J_{PC} = 15.7 Hz, ³J_{PC} = 7.7 Hz, ipso-C) ppm. ³¹P{¹H} NMR (C₆D₆, 121 MHz) δ 40.7 (d, ²J_{PP} = 179 Hz, PPh₂), 72.1 (d, ²J_{PP} = 179 Hz, P(*i*-Pr)₂) ppm. Anal. Calcd for C₁₈H₂₅NP₂: C, 68.13; H, 7.94; N, 4.41. Found: C, 68.21; H, 8.45; N, 4.27.

Zn[N(*i*-Pr₂P)₂]₂ (4). Diethylzinc (3.0 mL, 3.0 mmol, 1.0 M in hexanes) was added dropwise to a solution of **1** (1.50 g, 6.0 mmol) in ca. 15 mL anhydrous pentane. The colorless solution was allowed to stir overnight at rt before ca. half the solvent was removed under vacuum. The concentrated solution was cooled to −25 °C. Within 24 h, colorless crystals of **4** were formed and were isolated by decanting the supernatant solution. Yield = 1.15 g (68%), mp >200 °C. ¹H NMR (C₆D₆, 500 MHz) δ 1.17–1.27 (overlapping doublets, 48H, PCH(CH₃)₂), 1.89–1.95 (br sept, 8H, PCH(CH₃)₂) ppm. ¹³C{³¹P, ¹H} NMR (C₆D₆, 125 MHz) δ 17.9 (s, PCH(CH₃)₂), 19.1 (s, PCH(CH₃)₂), 29.4 (s, PCH(CH₃)₂) ppm. ³¹P{¹H} NMR (C₆D₆, 121 MHz) δ 91.4 ppm. Anal. Calcd for C₂₄H₅₆N₂P₄Zn: C, 51.29; H, 10.04; N, 4.98. Found: C, 51.60; H, 9.67; N, 4.80.

{EtZn[N(PPh₂)]₂}₂ (5). ZnEt₂ (3.4 mL, 3.4 mmol, 1.0 M in hexanes) was added slowly to a suspension of **2** (1.10 g, 2.85 mmol) in ca. 20 mL toluene. During the addition, the suspension became a colorless solution. The solution was allowed to stir overnight at rt before the solvent was removed under vacuum to give the white powder **5**. Yield = 1.29 g (98%), mp = 124 °C (dec). X-ray quality single crystals were grown from a concentrated 1:1:5 solution of toluene, THF and pentane. ¹H NMR (C₆D₆, 300 MHz) δ 0.32 (br, 4H, ZnCH₂CH₃), 1.05 (t, ³J_{HH} = 8.1 Hz, 6H, ZnCH₂CH₃), 6.94–7.05 (br m, 24H, meta/para C₆H₅), 7.46–7.58 (br m, 16 H ortho-C₆H₅) ppm. ¹³C{¹H} NMR (THF, 75 MHz) δ 7.0 (br, ZnCH₂CH₃), 12.0 (s, ZnCH₂CH₃), 128.1 (br s, meta-C), 128.8 (s, para-C), 132.8 (d, ²J_{CP} = 18 Hz, ortho-C), 141.8 (s, ipso-C) ppm. ³¹P{¹H} NMR (C₆D₆, 121 MHz) δ 49.7 ppm. Anal. Calcd for C₅₂H₅₀N₂P₄Zn₂: C, 65.22; H, 5.26; N, 2.93. Found: C, 65.14; H, 6.03; N, 2.74.

Zn[N(*i*-Pr₂P)(Ph₂P)]₂ (6). ZnEt₂ (1.6 mL, 1.6 mmol, 1.0 M in hexanes) was added to a solution of **3** (1.00 g, 3.2 mmol) in ca. 10 mL toluene. The colorless solution was heated to reflux under argon for 3 h. After cooling to rt, the solvent was removed under vacuum to give a white residue that was suspended in pentane and filtered. Yield = 0.67 g (61%), mp = 151–152 °C. X-ray quality single crystals were grown from a 1:1 mixture of pentane and THF. ¹H NMR (CD₂Cl₂, 300 MHz) δ 0.99 (br dd, 6H, CH(CH₃)₂), 1.16 (dd, ³J_{HH} = 7.2 Hz, ³J_{PH} = 14.8 Hz, 6H, CH(CH₃)₂), 2.02 (sept of d, ³J_{HH} = 7.2 Hz, ²J_{PH} = 14.0 Hz, 2H, CH(CH₃)₂), 7.31–7.35 (br m, 6H, meta/para C₆H₅), 7.47–7.54 (br m, 4H, ortho-C₆H₅) ppm. ¹³C{¹H} NMR (CD₂Cl₂, 75 MHz)

δ 17.0 (s, CH(CH₃)₂), 18.0–19.2 (vm, CH(CH₃)₂), 27.9 (vt, ¹J_{PC} = 18.3 Hz, CH(CH₃)₂), 128.0 (d, ³J_{CP} = 9.2 Hz, meta-C), 128.8 (s, para-C), 130.3 (d, ²J_{CP} = 13.9 Hz, ortho-C), 142.1 (dd, ¹J_{PC} = 26.1 Hz, ³J_{PC} = 19.0 Hz, ipso-C) ppm. ³¹P{¹H} NMR (CD₂Cl₂, 121 MHz) δ 62.1 (d, ²J_{PP} = 298 Hz, PPh₂), 101.3 (d, ²J_{PP} = 298 Hz, P(iPr)₂) ppm. Anal. Calcd for C₃₆H₄₈N₂P₄Zn: C, 61.94; H, 6.93; N, 4.01. Found: C, 62.54; H, 7.22; N, 3.86.

{EtZn[N(PPh₂)(i-Pr₂P)]₂} (7). A suspension of 3 (0.50 g, 1.58 mmol) in ca. 20 mL anhydrous pentane was added to a solution of ZnEt₂ (1.6 mL, 1.6 mmol, 1.0 M in hexanes) in ca. 10 mL pentane. The white suspension was allowed to stir overnight at rt before the solvent was removed under vacuum to give the white powder 7. Yield = 0.59 g (90%), mp = 147–150 °C. X-ray quality single crystals were grown from a concentrated pentane/THF solution. ¹H NMR (C₆D₆, 300 MHz) δ 0.35 (q, ³J_{HH} = 8.1 Hz, 4H, ZnCH₂CH₃), 1.02 (dd, ³J_{HH} = 6.9 Hz, ³J_{HP} = 17 Hz, 12H, CH(CH₃)₂), 1.03 (dd, ³J_{HH} = 6.9 Hz, ³J_{HP} = 12 Hz, 12H, CH(CH₃)₂), 1.30 (tt, ³J_{HH} = 8.1 Hz, ³J_{HP} = ⁴J_{HP} = 1.5 Hz, 6H, ZnCH₂CH₃), 2.56 (br sept, 4H, CH(CH₃)₂), 7.02–7.19 (br m, 12H, meta/para C₆H₅), 7.70–7.75 (m, 8H, ortho-C₆H₅) ppm. ¹³C{¹H} NMR (CD₂Cl₂, 75 MHz) δ 9.5 (d, ²J_{PC} = 58.8 Hz, ZnCH₂CH₃), 11.7 (s, ZnCH₂CH₃), 16.5 (d, ²J_{PC} = 4.6 Hz, CH(CH₃)₂), 17.9–18.9 (vm, CH(CH₃)₂), 25.4 (vt, ¹J_{PC} = 11.4 Hz, CH(CH₃)₂), 128.0 (d, ³J_{PC} = 5.3 Hz, meta-C), 128.1 (s, para-C), 131.7 (d, ²J_{PC} = 20.8 Hz, ortho-C), 145.5 (d, ¹J_{PC} = 19.0 Hz, ipso-C) ppm. ³¹P{¹H} NMR (C₆D₆, 121 MHz) δ 52.3 (s, PPh₂), 71.4 (s, P(i-Pr)₂) ppm. Anal. Calcd for C₄₀H₅₈N₂O₂P₄Zn₂: C, 58.48; H, 7.12; N, 3.41. Found: C, 57.45; H, 7.10; N, 3.73.

Zn[O₂CP(i-Pr)₂NP(i-Pr)₂]₂ (8). Carbon dioxide was bubbled through a solution of 3 (0.50 g, 0.89 mmol) in ca. 10 mL pentane for 15 min. The white precipitate that formed was separated by filtration through a glass frit. Yield = 0.46 g (79%), mp = 98–99 °C. X-ray quality crystals were grown at –25 °C from the concentrated supernatant solution. ¹H NMR (C₆D₆, 300 MHz) δ 1.13 (br, 24H, O₂CPCH(CH₃)₂), 1.18 (d, ³J_{HH} = 7.2 Hz, 12H, PCH(CH₃)₂), 1.23 (d, ³J_{HH} = 7.2 Hz, 12H, PCH(CH₃)₂), 1.68 (br, 2H, O₂CPCH(CH₃)₂), 1.92 (br, 2H, O₂CPCH(CH₃)₂), 2.13–2.26 (overlapping sept, 4H, PCH(CH₃)₂) ppm. ¹³C{¹H} NMR (C₆D₆, 125 MHz) δ 15.9–19.3 (overlapping br, CH₃), 25.6–28.9 (overlapping br, CH), 168.8 (d, ¹J_{CP} = 90 Hz, O₂CP) ppm. ³¹P{¹H} NMR (C₆D₆, 121 MHz) δ 31.6 (s, O₂CP(i-Pr)₂), 45.8 (s, P(i-Pr)₂) ppm. IR (nujol mull) ν 1633 (s) cm⁻¹. Anal. Calcd for C₂₆H₅₆N₂O₄P₄Zn: C, 48.04; H, 8.68; N, 4.31. Found: C, 48.09; H, 8.67; N, 4.15.

N(PPh₂)₃ (9). Carbon dioxide was bubbled through a solution of 5 (0.20 g, 0.21 mmol) in ca. 10 mL toluene for 15 min. The white precipitate 9 was isolated by filtration. Yield = 0.07 g (68%), mp = 195–197 °C. X-ray quality single crystals were grown from a concentrated toluene solution and were found to be identical to the previously reported N(PPh₂)₃.¹³ ³¹P{¹H} NMR (toluene, 121 MHz) δ 59 ppm.

Ph₂P(iPr)₂NPPh₂ (10). Carbon dioxide was bubbled through a solution of 6 (0.25 g, 0.36 mmol) in ca. 10 mL THF for 15 min. Solvent was removed under vacuum to give a colorless oil that was then dissolved in 2 mL of a 1:1 mixture of THF and pentane. The solution was cooled to –25 °C and colorless crystals of 10 were isolated after several days by decanting the supernatant solution. mp = 121 °C. ¹H NMR (CD₂Cl₂, 300 MHz) δ 1.13 (dd, ²J_{PH} = 16 Hz, ³J_{HH} = 7.2 Hz, 6H, CH(CH₃)₂), 1.23 (dd, ²J_{PH} = 16 Hz, ³J_{HH} = 7.2 Hz, 6H, CH(CH₃)₂), 2.45 (br sept of d, ³J_{HH} = 7.2 Hz, 2H, CH(CH₃)₂), 7.25–7.85 (br m, 20H, C₆H₅) ppm. ¹³C{¹H} NMR (CD₂Cl₂, 75 MHz) δ 17.4 (s, CH₃), 29.9 (d, ¹J_{CP} = 49 Hz, CH), 127.2 (s, aryl-C), 127.6 (d, ¹J_{CP} = 6 Hz, aryl-C) 128.4 (d, ¹J_{CP} = 8 Hz, aryl-C), 129.6 (d, ¹J_{CP} = 12 Hz, aryl-C), 129.9 (s, aryl-C), 135.9 (d, ¹J_{CP} = 20 Hz, aryl-C) ppm (ipso C not observed). ³¹P{¹H} NMR (CD₂Cl₂, 121 MHz) δ –29.7 (d, ¹J_{PP} = 267 Hz, Ph₂P-P(iPr)₂), 39.7 (d, ²J_{PP} = 82 Hz, NPPPh₂), 44.5 (dd, ¹J_{PP} = 267 Hz, ²J_{PP} = 82 Hz, P(iPr)₂) ppm. Anal. Calcd for C₃₀H₃₄NP₃: C, 71.85; H, 6.83; N, 2.79. Found: C, 71.26; H, 7.68; N, 2.59.

Zn[O₂CP(i-Pr)₂NPPh₂][Ph₂PN(i-Pr)₂]ZnEt₂ (11). Carbon dioxide was bubbled through a suspension of 7 (0.15 g, 0.18 mmol) in ca. 15 mL pentane for 15 min. The white precipitate was then isolated by filtration through a glass frit. Yield = 0.14 g (87%), mp = 108–110 °C. X-ray quality crystals were grown by vapor diffusion of pentane into a

concentrated toluene solution. ¹H NMR (C₆D₆, 300 MHz) δ 0.42–0.54 (br m, 4H, ZnCH₂CH₃), 0.81–1.42 (overlapping dd, 24H, CH(CH₃)₂), 1.53–1.66 (br, 3H, O₂CZnCH₂CH₃), 1.84 (t, ³J_{HH} = 8 Hz, 3H, ZnCH₂CH₃), 2.28–2.33 (br, 3 H, CH(CH₃)₂), 2.76–2.81 (br, 1H, CH(CH₃)₂), 6.89–7.30 (overlapping m, 12H, C₆H₅), 7.78–7.92 (overlapping m, 8H, C₆H₅) ppm. ¹³C{¹H} NMR (C₆D₆, 75 MHz) δ –1.8 (br s, ZnCH₂), 13.1 (s, CH₃), 13.9 (s, CH₃), 15.4 (s, CH₃), 16.4 (s, CH₃), 24.6 (br s, CH(CH₃)₂), 25.3 (br s, CH(CH₃)₂), 128.7 (s, aryl-C), 131.7 (s, aryl-C), 131.9 s, aryl-C), 143.1 (s, aryl-C) ppm. CO₂ signal not observed. ³¹P{¹H} NMR (C₆D₆, 121 MHz) δ 23.2 (dd, ²J_{PP} = 94.0 Hz, ²J_{PP} = 31.2 Hz, ZnPPh₂), 37.1 (d, ²J_{PP} = 31.2 Hz, O₂CP(i-Pr)₂), 53.2 (d, J = 6.2 Hz, PPh₂), 66.0 (d, ²J_{PP} = 94.0 Hz, P(i-Pr)₂) ppm. IR (nujol mull) ν 1634 (s) cm⁻¹. Anal. Calcd for C₄₁H₅₈N₂O₂P₄Zn₂: C, 56.89; H, 6.75; N, 3.24. Found: C, 56.59; H, 7.02; N, 2.51.

■ ASSOCIATED CONTENT

Supporting Information

CIF files for 3–8, 10, and 11. Crystallographic data tables and figures showing cocrystallized solvent in 5 and 7 and both independent molecules of 8. This material is available free of charge via the Internet at <http://pubs.acs.org>. The CIF files have also been deposited at the CCDC (1017724–1017731).

■ AUTHOR INFORMATION

Corresponding Author

* E-mail: rakemp@unm.edu.

Notes

The authors declare no competing financial interest.

■ ACKNOWLEDGMENTS

This work was financially supported by the National Science Foundation (Grant CHE12-13529) and by the Laboratory Directed Research and Development (LDRD) program at Sandia National Laboratories (LDRDs 14938 and 151300). D.A.D. was financially supported by the Natural Sciences and Engineering Research Council (NSERC) of Canada by means of a Postdoctoral Fellowship. The Bruker X-ray diffractometer was purchased via a National Science Foundation CRIF:MU award to the University of New Mexico (CHE04-43580), and the NMR spectrometers were upgraded via grants from the NSF (CHE08-40523 and CHE09-46690). Sandia is a multi-program laboratory operated by Sandia Corporation, a Lockheed Martin Company, for the United States Department of Energy under Contract No. DE-AC04-94AL85000.

■ REFERENCES

- (1) (a) Aresta, M.; Dibenedetto, A.; Angelini, A. *Chem. Rev.* **2014**, *114*, 1709. (b) Qiao, J.; Liu, Y.; Hong, F.; Zhang, J. *Chem. Soc. Rev.* **2014**, *43*, 631. (c) Costentin, C.; Robert, M.; Savéant, J.-M. *Chem. Soc. Rev.* **2013**, *42*, 2423. (d) Appel, A. M.; Bercaw, J. E.; Bocarsly, A. B.; Dobbek, H.; Dubois, D. L.; Dupuis, M.; Ferry, J. G.; Fujita, E.; Hille, R.; Kenis, P. J. A.; Kerfeld, C. A.; Morris, R. H.; Peden, C. H. F.; Portis, A. R.; Ragsdale, S. W.; Rauchfuss, T. B.; Reek, J. N. H.; Seefeldt, L. C.; Thauer, R. K.; Waldrop, G. L. *Chem. Rev.* **2013**, *113*, 6621. (e) Hoffmann, M. R.; Moss, J. A.; Baum, M. M. *Dalton Trans.* **2011**, *40*, 5151. (f) Olah, G. A.; Prakash, G. K.; Goepfert, A. *J. Am. Chem. Soc.* **2011**, *133*, 12881. (g) Wang, W.; Wang, S.; Ma, X.; Gong, J. *Chem. Soc. Rev.* **2011**, *40*, 3703. (h) Mikkelsen, M.; Jørgensen, M.; Krebs, F. *Energy Environ. Sci.* **2010**, *3*, 43. (i) Olah, G. A.; Goepfert, A.; Prakash, G. K. *J. Org. Chem.* **2009**, *74*, 487. (j) Benson, E. E.; Kubiak, C. P.; Sathrum, A. J.; Smieja, J. M. *Chem. Soc. Rev.* **2009**, *38*, 89.
- (2) (a) McCahill, J. S. J.; Welch, G. C.; Stephan, D. W. *Angew. Chem., Int. Ed.* **2007**, *46*, 4968. (b) Welch, G. C.; Cabrera, L.; Chase, P. A.;

Hollink, E.; Masuda, J. D.; Wei, P.; Stephan, D. W. *Dalton Trans.* **2007**, 3407.

(3) Allen, F. H. *Acta Crystallogr., Sect. B: Struct. Sci.* **2002**, *58*, 380 (CSD version 5.35, May 2014 update).

(4) (a) Ménard, G.; Gilbert, T. M.; Hatnean, J. A.; Kraft, A.; Krossing, I.; Stephan, D. W. *Organometallics* **2013**, *32*, 4416. (b) Stephan, D. W.; Erker, G. *Angew. Chem., Int. Ed.* **2010**, *49*, 46. (c) Lim, C.-H.; Holder, A. M.; Hynes, J. T.; Musgrave, C. B. *Inorg. Chem.* **2013**, *52*, 10062.

(5) Dickie, D. A.; Coker, E. N.; Kemp, R. A. *Inorg. Chem.* **2011**, *50*, 11288.

(6) (a) Rheingold, A. L. Private communication, *Cambridge Structural Database*; **2005**; CIXSAD01. (b) Nöth, H.; Meinel, L. Z. *Anorg. Allg. Chem.* **1967**, *349*, 225. (c) Nöth, H.; Fluck, E. Z. *Naturforsch., B: Chem. Sci.* **1984**, *39*, 744.

(7) Dickie, D. A.; Gislason, K. B.; Kemp, R. A. *Inorg. Chem.* **2012**, *51*, 1162.

(8) (a) Dulai, A.; McMullin, C. L.; Tenza, K.; Wass, D. F. *Organometallics* **2011**, *30*, 935. (b) Eichhorn, B.; Nöth, H.; Seifert, T. *Eur. J. Inorg. Chem.* **1999**, 2355.

(9) (a) Majoumo-Mbé, F.; Köhl, O.; Lönnecke, P.; Silaghi-Dumitrescu, I.; Hey-Hawkins, E. *Dalton Trans.* **2008**, 3107. (b) Majoumo-Mbé, F.; Lönnecke, P.; Hey-Hawkins, E. *Organometallics* **2005**, *24*, 5287. (c) Olbert, D.; Görls, H.; Conrad, D.; Westerhausen, M. *Eur. J. Inorg. Chem.* **2010**, 1791.

(10) (a) Wingerter, S.; Pfeiffer, M.; Baier, F.; Stey, T.; Stalke, D. Z. *Anorg. Allg. Chem.* **2000**, *626*, 1121. (b) Dickie, D. A.; Ulibarri-Sanchez, R. P., III; Jarman, P. J.; Kemp, R. A. *Polyhedron* **2013**, *58*, 92.

(11) (a) Mömmling, C. M.; Otten, E.; Kehr, G.; Fröhlich, R.; Grimme, S.; Stephan, D. W.; Erker, G. *Angew. Chem., Int. Ed.* **2009**, *48*, 6643. (b) Boudreau, J.; Courtemanche, M.-A.; Fontaine, F.-G. *Chem. Commun.* **2011**, *47*, 11131. (c) Zhao, X.; Stephan, D. W. *Chem. Commun.* **2011**, *47*, 1833. (d) Peuser, I.; Neu, R. C.; Zhao, X.; Ulrich, M.; Schirmer, B.; Tannert, J. A.; Kehr, G.; Fröhlich, R.; Grimme, S.; Erker, G.; Stephan, D. W. *Chem.—Eur. J.* **2011**, *17*, 9640. (e) Roters, S.; Appelt, C.; Westenberg, H.; Hepp, A.; Slootweg, J. C.; Lammertsma, K.; Uhl, W. *Dalton Trans.* **2012**, *41*, 9033. (f) Chapman, A. M.; Haddow, M. F.; Wass, D. F. *J. Am. Chem. Soc.* **2011**, *133*, 18463. (g) Harhausen, M.; Fröhlich, R.; Kehr, G.; Erker, G. *Organometallics* **2012**, *31*, 2801.

(12) (a) Ménard, G.; Stephan, D. W. *Angew. Chem., Int. Ed.* **2011**, *50*, 8396. (b) Bertini, F.; Lyaskovskyy, V.; Timmer, B. J. J.; de Kanter, F. J. J.; Lutz, M.; Ehlers, A. W.; Slootweg, J. C.; Lammertsma, K. *J. Am. Chem. Soc.* **2012**, *134*, 201.

(13) Ellermann, J.; Köck, E.; Zimmermann, H.; Gomm, M. *Acta Crystallogr., Sect. C: Cryst. Struct. Commun.* **1987**, *C43*, 1795.

(14) (a) Dickie, D. A.; Kemp, R. A. *Acta Crystallogr., Sect. E: Struct. Rep. Online* **2008**, *E64*, o1449. (b) Dickie, D. A.; Parkes, M. V.; Kemp, R. A. *Angew. Chem., Int. Ed.* **2008**, *47*, 9955.

(15) (a) Sushev, V. V.; Kornev, A. N.; Kurskii, Y. A.; Kuznetsova, O. V.; Fukin, G. K.; Budnikova, Y. H.; Abakumov, G. A. *J. Organomet. Chem.* **2005**, *69*, 1814. (b) Braunstein, P.; Hasselbring, R.; Tiripicchio, A.; Ugozzoli, F. J. *Chem. Soc., Chem. Commun.* **1995**, 37. (c) Ellermann, J.; Sutter, J.; Knoch, F. A.; Moll, M. *Angew. Chem., Int. Ed.* **1993**, *32*, 700. (d) Ellermann, J.; Sutter, J.; Schelle, C.; Knoch, F. A.; Moll, M. Z. *Anorg. Allg. Chem.* **1993**, *619*, 2006. (e) Ellermann, J.; Gabold, P.; Schelle, C.; Knoch, F. A.; Moll, M.; Bauer, W. Z. *Anorg. Allg. Chem.* **1995**, *621*, 1832. (f) Dotzler, M.; Schmidt, A.; Ellermann, J.; Knoch, F. A.; Moll, M.; Bauer, W. *Polyhedron* **1996**, *15*, 4425.

(16) Elder, P. J. W.; Chivers, T.; Thirumoorthi, R. *Eur. J. Inorg. Chem.* **2013**, *2013*, 2867.